ARPHA Proceedings

Proceedings CAUSummit 2025, 0099-0105
doi: 10.3897/ap.9.e0099

10th Anniversary
World Summit: Civil Engineering-Architecture-Urban Planning Congress

Design Blast Factors Assessment and its Effect on Rock Fragmentation at Limestone Quarry, Setif, Algeria

Mohamed Fredj[1, a)], Riadh Boukarm [1,2], Abderrazak Saadoun [1], Kamel Menacer [3], Radouane Nakache [3]

[1] *University of Bejaia, Faculty of Technology, Mining and Geology Department, 06000 Bejaia, Algeria*
[2] *University of Bejaia, Faculty of Technology, Construction Engineering and Architecture Laboratory (LGCA), 06000 Bejaia, Algeria*
[3] *University of Badji Mokhtar Annaba, Faculty of Earth Science, Mining Department, 12000 Annaba, Algeria*

[a)] Corresponding author: mohamed.fredj@univ-bejaia.dz

Abstract. Blasting outcomes significantly impact all subsequent operations in quarrying and mining. The factors affecting blasting results are categorized as controllable, such as blast geometry and explosive characteristics, or non-controllable, including geological conditions and regulatory requirements. Achieving optimal fragmentation requires careful adjustment of controllable parameters to align with non-controllable parameters. This study analyzed four distinct blast designs by examining the influence of blast design parameters on rock fragmentation. Rock samples from each blast face were tested, and digital images of the resulting muckpiles were processed using WipFrag 3.3 software to assess the fragmentation. Particle size distributions (PSD) were established for each blast, and mean particle fragment sizes (MeanPS) were correlated with the respective blast design parameters. For a gyratory crusher with a 1200 mm feed size, the percentage cumulative passing ranged from 89.1%–100%. The study found strong correlations between MeanPS and factors such as the stiffness ratio and powder factor (PF). Specifically, MeanPS increased with the stiffness ratio (correlation coefficient: 76.13%) and decreased as PF increased (correlation coefficient: 98.74%). Conversely, the spacing-to-burden ratio had a minimal effect on the fragment size. All four-blast events studied produced good fragmentation, with a uniformity index ranging from 1.16 to 1.61. The study concluded that blast design parameters significantly influence rock fragmentation. The stiffness ratio and PF showed a high correlation with MeanPS. Regular assessment and optimization of these parameters can enhance the efficiency and productivity of quarrying operations in the long term.

Keywords: Blasting; fragmentation; limestone quarry; Djebel Medjounes; powder factor; spacing to burden ratio.

INTRODUCTION

Drilling and Blasting parameters are specific to each quarry, and their influence on rock fragmentation is a key consideration when developing a blasting plan. Fragment size is a primary measure for assessing the efficiency and productivity of blasting operations [1-7]. Without the regular evaluation of rock fragmentation, quarrying processes may face higher production costs and unexpected delays. Since drilling and blasting make up 20% of total mining expenses [8], optimizing blast design is essential for improving quarrying efficiency.

When blasting does not achieve the intended fragment size, operational costs can increase because of the need for additional secondary blasting and slower material handling [9]. Effective blasting enhances the performance of loaders and excavators by increasing the bucket and truck fill rates and improving the ease of excavation [10, 11]. Consistent fragment sizes also boost crusher and mill throughput while reducing the energy required for the comminution.

Although higher explosive charges may increase the initial drilling and blasting costs, they can lower the expenses of subsequent processes by producing finer fragments [12]. However, the overuse of explosives should be avoided to prevent environmental harm and excessive fine generation.

The powder Factor (PF), burden distance (Bd), and height of the bench (Hb) are the three main controllable variables that impact the fragmentation distribution. Fragment size and muck-pile shape are susceptible to Bd during bench blasting [13, 14]. The PF is primarily determined by the rock characteristics, such as discontinuities, strength, and lithology [15-17]. Generally, increasing the PF yields smaller fragments if the rock properties remain unchanged [8, 17].

Singh et al. [18] found that particle fragment size increases with greater Bd and Hb. Combining field data with theoretical analyses is recommended for more accurate fragmentation predictions rather than relying solely on mechanical models [14, 16]. This integrated approach enables the development of reliable and site-specific prediction models.

GENERAL SETTING OF DJEBEL MEDJOUNES QUARRY

This study was conducted at the Djebel Medjounes Quarry, located in Ain El-Kebira, 20 km northeast of Setif, Algeria. Figure 1 illustrates the location of the Djebel Medjounes Quarry in Ain El-Kebira, Setif, Algeria[5, 19].

FIGURE 1. Location map of the study quarry in Ain El-Kebira, Setif, Algeria [5].

The study area has a longitude of 5°27'E, a latitude of 36°20' N, and an altitude of 1040 m. The quarry produces approximately 2.2 MT of limestone annually. A very pronounced relief characterizes this deposit, extending over 15 km from east to west, with an average width of 7 km, reaching an altitude of 1461 m at the peak. The limestone rock is medium-hard, and the upper part of the limestone deposit is intensely fractured, which poses problems of hole clogging during drilling and the quality of filling [5].

MATERIALS AND METHODS

The key blast design parameters were recorded for four separate blasting events. Post-blast, images of the muck-piles were captured using an appropriate camera to facilitate the fragmentation analysis. The PSD charts were generated based on the measured sizes of the fragmented rocks. The data from the fragmentation analysis were evaluated and compared to the blast design parameters.

Data of Design Blast

Data was collected from four observed blast events. Bulk explosives with a density of 1.05 g/cm³ were used as the blasting agent. The diameter and depth of the hole, spacing, burden, explosive weight per hole, density charging, and stemming length were also calculated. The blastholes ranged from 15 to 16.5 m in depth, with a slope angle of 8°. Bulk explosives with an open cup density of 1 g/cm³ and a detonation velocity of 4500 m/s at a hole diameter of 110 mm were used.

Fragmentation Analysis

Digital image processing was employed to assess the size distribution of blasted rock fragments, and it was chosen for its efficiency, cost-effectiveness, and speed of analysis [6]. WipFrag 3.3 software was used for the analysis. Images of the muck-piles from four blast events were captured using a digital camera and transferred to WipFrag 3.3 software. Each image was scaled using a ball with a diameter of 20 cm. Delineation and edge detection processes were applied to produce a net for the analysis. The PSD charts were then produced.

Powder Factor

The PF represents the ratio of explosive weight to the volume of rock blasted. It was calculated for each blast using Eq. 1:

$$PF = Q_h / V \tag{1}$$

Where ***We*** is the weight of explosive per blasthole (kg), and ***V*** is the volume of rock blasted per hole (m³)

The total explosive used in each hole ($\boldsymbol{Q_h}$) is the sum of the primer charge (***P***) and the column charge ($\boldsymbol{Q_c}$), as shown in Eq. 2:

$$Q_h = P + Q_c \tag{2}$$

The column charge ($\boldsymbol{Q_c}$) in kilograms was determined using Eq. 3:

$$Q_c = 0.785 \times D^2 \times Lc \times \rho \tag{3}$$

Where ***D*** is the diameter of the hole (m), Lc is the length of the charge (m), and $\boldsymbol{\rho}$ is the explosive density (kg/m³). The volume (***V***) of the rock blasted per hole was determined using Eq. 4:

$$V = B \times S \times Hb \tag{4}$$

where ***B*** is the burden (m), S is the spacing between the two holes (m), and Hb is the height of the bench (m). The height of the bench was determined by subtracting the subdrill length (***SD***) from the hole depth (***L***) and multiplying by the slope angle (β), as given in Eq. 5:

$$Hb = (L - SD)cos\beta \tag{5}$$

RESULTS AND DISCUSSION

Blast Design Parameters

Table 1 presents the blast design parameters recorded for each of the blasts. The PF ranged from 0.44 to 0.57 kg/m³, whereas the detonated explosive charge per hole varied between 109.67 and 124.62 kg. All four explosions maintained a consistent burden. Eqs. 2 to 5 provide further details regarding these parameters.

TABLE 1. Design Parameters of the Blast.

Parameters	B1	B2	B3	B4
Hole Diameter (m)	0.11	0.11	0.11	0.11
Hole depth (m)	15.5	16	15	16.5
Spacing (m)	3.5	4	4.5	4.5
Stemming (m)	4	4	4	4
Burden (m)	4	4	4	4
Subdrill (m)	1.1	1.3	1.1	1.5
Explosive per Hole (Kg/hole)	114.65	119.64	109.67	124.62
Powder Factor (kg/m^3)	0.57	0.51	0.44	0.46
Volume blasted (m^3)	199.5	232.8	247.68	267.3

Figure 2 illustrates the particle fragment size distribution charts generated by the image processing WipFrag 3.3 software for each blast round. Each chart has four main sections: the left panel displays the key measurement data and percentage passing values. Adjacent to this, the sizes of the sieves and their corresponding cumulative percentages of fragments passing. The middle area features a blue curve representing the percentage of passing fragments. The horizontal axis is shown on a logarithmic scale.

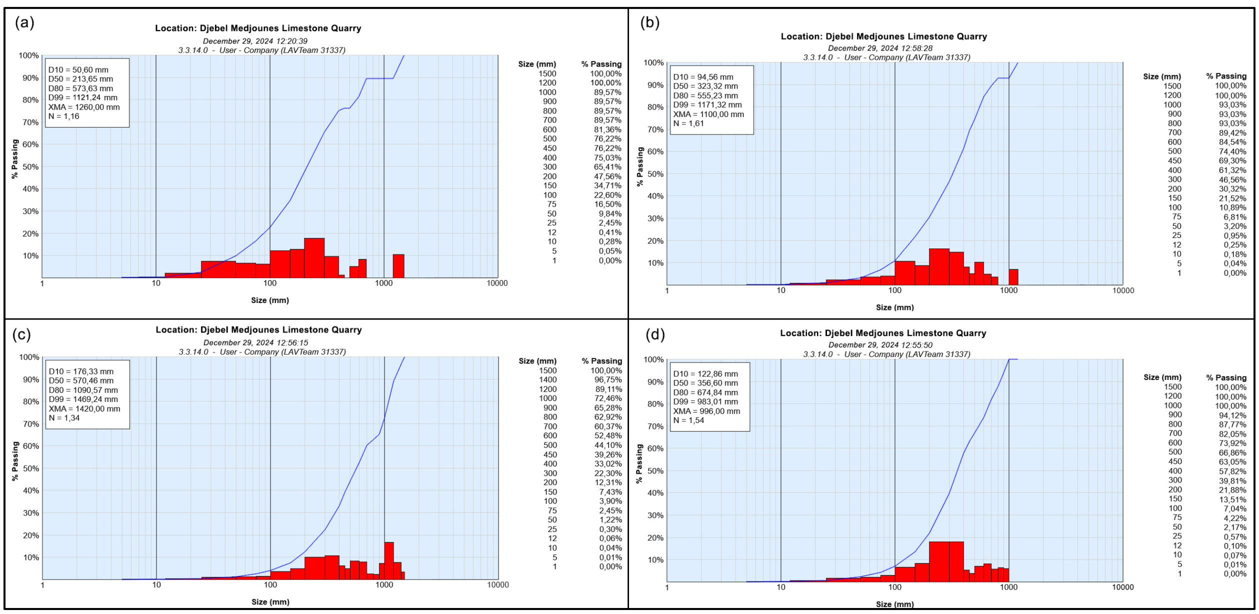

FIGURE 2. Particle fragment size distribution analysis for (a) blast 1, (b) blast 2, (c) blast 3, and (d) blast 4.

TABLE 2. Details of the distribution of the particle fragment sizes.

Parameters	B1	B2	B3	B4
MinPS(mm)	1.16	0.95	1.52	0.83
MaxPS(mm)	1260.00	1100.00	1420.00	996.00
MeanPS (mm)	52.49	83.20	112.920	98.87
D10 (mm)	50.60	94.56	176.33	122.86
D50 (mm)	213.65	323.32	570.46	356.60
D80 (mm)	573.63	555.23	1090.57	674.84
Uniformity index (n)	1.16	1.61	1.34	1.54
% passing at 1200 mm	100.00	100.00	89.11	100.00

At the Djebel Medjounes Quarry, the primary crusher used is a gyratory with a maximum feed size of 1200 mm. Table 2 summarizes the PSD and other fragmentation analysis details of the samples. It lists the MinPS, MaxPS, and MeanPS values for each blast. D10, D50, and D80 denote the sizes of the sieves through which 10%, 50%, and 80% of the fragmented material passed, respectively. The uniformity index (n) reflects how closely the fragments align with the MeanPS [20, 21].

Across all four blasts, the MeanPS ranged from 52.49 to 112.92 mm. MaxPS for four blasts were below 1200 mm (crusher's gape), resulting in 100% passing and no oversize, except for blast 3, which produced a Max.PS of 1420 mm and led to 89.11% passing with 10.89% oversize.

Blasting Design Factors and Mean Fragment Particle Size

Table 3 lists the blasting design parameters and MeanPS values of the corresponding muck-piles for all blasts. Blast 1 had the highest PF (0.57 kg/m³) and the smallest MeanPS (52.49 mm), while blast 3 had the lowest PF (0.44 kg/m³) and the largest MeanPS (112.92 mm).

TABLE 3. Design parameters and MeanPS

Blasts	S/B ratio	Stiffness ratio (Sr)	PF (kg/m^3)	MeanPS (mm)
B1	1.125	3.75	0.57	52.49
B2	0.875	3.875	0.51	83.2
B3	1	4.025	0.44	112.92
B4	1.125	4.125	0.46	98.87

Figure 3 illustrates the relationship between the blast design factors and MeanPS. Figure 3a demonstrates that the S/B ratio is insignificant in determining the MeanPS of blast designs. In Table 3, blasts 1 and 4 share the same S/B ratio of 1.125, yet their MeanPS values vary. The MeanPS of blast 1 (52.49 mm) compared to that of blast 4 (98.87 mm) with the same S/B ratio can be attributed to the low powder factor. Proper burden prevents rapid gas release and insignificant fragmentation, while appropriate spacing avoids over-crushing and insufficient fracturing [17].

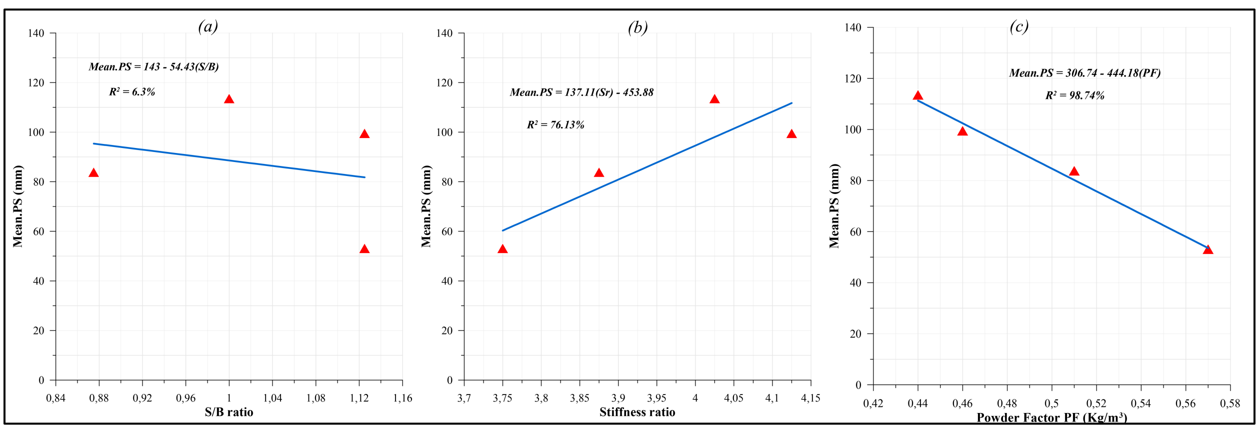

FIGURE 3. Regression analysis, (a) MFS and spacing-burden ratio, (b) MFS and stiffness ratio, and(c) MFS and PF

The stiffness ratio (Sr) significantly affects MeanPS, with a coefficient of 76.13% (Figure 3b). Higher stiffness ratios result in coarser fragments, and excessively high ratios can cause poor fragmentation.

Figure 3c reveals a correlation coefficient of 98.74% between PF and MeanPS, indicating that the fragment size is strongly influenced by the charge of the explosives used, with higher PF yielding finer fragments. However, the explosive quantity is also determined by the hole diameter, rock strength, and water conditions of the site. These results are consistent with previous studies [16, 17, 22].

CONCLUSIONS

This study examined how blast design factors influence mean particle fragment size. The stiffness ratio (Sr) and PF are key determinants of the fragment particle size. The mean particle fragment size increased with the stiffness ratio but decreased as the PF increased. A higher PF produces finer fragments, whereas the spacing-to-burden ratio has little effect on the mean size.

In this study at Djebel Medjounes quarry, using a PF of 0.44–0.57 kg/m³, a spacing of 3.5 or 4.5 m, and a burden of 4 m resulted in 89.11% to 100% cumulative passing for all four blasts, with oversize occurring only in blast 3 (10.89%). The mean particle fragment sizes ranged from 52.49 to 112.92 mm, all suitable for the 1200 mm primary crusher opening, indicating effective ore fragmentation.

As only four blasts were analysed, further research involving more blast events is recommended to validate these findings under current quarry practices and geological conditions. Future studies should also consider other rock mass characteristics, such as the influence of discontinuities (orientation & spacing), and the explosive properties.

REFERENCES

1. M. Fredj, R. Boukarm, A. Saadoun, K. Menacer, and R. Nakache, "Effect of Stemming Parameters on Blast-Induced Rock Fragmentation: A Case Study," ARPHA Proceedings, vol. **7**, pp. 128–135, (2024). https://doi.org/10.3897/ap.7.e0128
2. A. Saadoun, R. Boukarm, M. Fredj, K. Menacer, D. Boudjellal, A. Hafsaoui, and I. Yilmaz, "Optimal Blast Design Considering the Effects of Geometric Blasting Parameters on Rock Fragmentation: A Case Study," ARPHA Proceedings, vol. 7, pp. 136–146, (2024). https://doi.org/10.3897/ap.7.e0136
3. A. Saadoun, R. Boukarm, M. Fredj, and Y. Isik, "Study The Influence of The Choice of Blasting Zones on The Rock Fragmentation Quality and The Stability of Benches in Open-Pit Mining by Numerical Modeling," in Proc. SGEM, pp. 439–446, (2023). https://doi.org/10.5593/sgem2023/1.1/s03.53
4. M. Fredj, R. Boukarm, R. Nakache, A. Saadoun, M. Saoudi, and I. Tighilt, "Distribution Analysis of Rock Fragments Size Based on the Digital Image Processing and the Kuz-Ram Model. Case of Jebel Medjounes Quarry," Aspects Min. Miner. Sci., vol. 2, no. 4, (2019).https://doi.org/10.31031/AMMS.2019.02.000545
5. A. Saadoun, M. Fredj, R. Boukarm, and H. Riheb, "Fragmentation analysis using digital image processing and empirical model (Kuz-Ram): a comparative study," J. Min. Inst., vol. 257, pp. 822–832, (2022). https://doi.org/10.31897/PMI.2022.84
6. B. S. Choudhary, "Firing patterns and their effect on muckpile shape parameters and fragmentation in quarry blasts," Int. J. Res. Eng. Technol., vol. 2, no. 9, pp. 32–45, (2013).
7. B. Elevli, I. Topal, and S. Elevli, "Multivariate statistics application in development of blast fragmentation charts for different rock formations in quarries," Acta Montan. Slovaca, vol. 17, no. 4, pp. 300–309, (2012).
8. S. Prasad, B. S. Choudhary, and A. K. Mishra, "Effect of stemming to burden ratio and powder factor on blast induced rock fragmentation– a case study," IOP Conf. Ser.: Mater. Sci. Eng., vol. 225, (2017). https://doi.org/10.1088/1757-899X/225/1/012191
9. P. H. S. W. Kulatilake, Q. Wu, T. Hudaverdi, and C. Kuzu, "Mean particle size prediction in rock blast fragmentation using neural networks," Eng. Geol., vol. 114, no. 3–4, pp. 298–311, (2010). https://doi.org/10.1016/j.enggeo.2010.05.008
10. B. Bozic, "Control of fragmentation by blasting," Rudarsko-Geolosko-Naftni Zbornik, vol. 10, no. 1, pp. 49–57, (1998).
11. S. S. Kanchibotla, S. Morrell, W. Valery, and P. O'Loughlin, "Exploring the effect of blast design on SAG mill throughput at KCGM," in Proc. Mine to Mill Conf., Australasian Inst. Min. Metall., Brisbane, QLD, pp. 153–158, (1998).
12. L. Workman and J. Eloranta, "The effects of blasting on crushing and grinding efficiency and energy consumption," in Proc. 29th Annu. Conf. Explosives and Blasting Technique, Int. Soc. Explosive Eng., Nashville, TN, pp. 1–5, (2003).
13. P. Yan, W. Zhou, W. Lu, M. Chen, and C. Zhou, "Simulation of bench blasting considering fragmentation size distribution," Int. J. Impact Eng., vol. 90, pp. 132–145, (2016). https://doi.org/10.1016/j.ijimpeng.2015.11.015
14. P. A. Persson, R. Holmberg, and J. Lee, Rock Blasting and Explosives Engineering. Boca Raton, FL:

CRC Press, (1994). https://doi.org/10.1201/9780203740514

15. M. Ruest, P. Cundall, A. Guest, and G. Chitombo, “Developments using the particle flow code to simulate rock fragmentation by condensed phase explosives,” in Proc. 8th Int. Symp. Rock Fragmentation by Blasting (Fragblast 8), Santiago, Chile, pp. 140–151, (2006).
16. S. S. Kanchibotla, W. Valery, and S. Morrell, “Modelling fines in blast fragmentation and its impact on crushing and grinding,” in Explo'99: A Conf. Rock Breaking, Aust. Inst. Min. Metall., Kalgoorlie, WA, pp. 137–144, (1999).
17. F. Mohamed, A. Hafsaoui, K. Talhi, and K. Menacer, “Study of the powder factor in surface bench blasting,” Procedia Earth Planet. Sci., vol. 15, pp. 892–899, (2015). https://doi.org/10.1016/j.proeps.2015.08.142
18. P. K. Singh, M. P. Roy, R. K. Paswan, S. Kumar, and R. R. Jha, “Rock fragmentation control in opencast blasting,” J. Rock Mech. Geotech. Eng., vol. 8, no. 2, pp. 225–237, (2016). https://doi.org/10.1016/j.jrmge.2015.10.005
19. Z. Karim, R. Hadji, and Y. Hamed, “GIS-based approaches for the landslide susceptibility prediction in Setif Region (NE Algeria),” Geotech. Geol. Eng., vol. 37, no. 1, pp. 359–374, (2019). https://doi.org/10.1007/s10706-018-0615-7
20. C. V. B. Cunningham, “The Kuz-Ram model for prediction of fragmentation from blasting,” in R. Holmberg and A. Rustan, Eds., 1st Int. Symp. Rock Fragmentation, Div. Min. Rock Excavation, Lulea Univ. Technol., Lulea, Sweden, pp. 439–454, (1983).
21. C. V. B. Cunningham, “Fragmentation estimations and the Kuz–Ram model - four years on,” in W. L. Fourney and R. D. Dick, Eds., 2nd Int. Symp. Rock Fragmentation by Blasting, Soc. Exp. Mech., Keystone, CO, pp. 475–487, (1987).
22. P. K. Singh, M. P. Roy, R. K. Pasawan, Md. Sarim, and S. Kumar, “Blast design and fragmentation control - Key to productivity,” J. Mines, Metals Fuels, vol. 63, no. 7, pp. 182–189, (2015).